Presented at:
1982 Nuclear Science Symposium,
Washington, D.C., October 19-22, 1982

BNL 32208

CONF-821011--39

BNL--32208

DE83 004603

CHARGE COLLECTION IN SILICON STRIP DETECTORS*

H. W. Kraner, R. Beuttenmuller, T. Ludlam, A. L. Hanson,
K. W. Jones, and V. Radeka
Brookhaven National Laboratory, Upton, New York 11973

E. H. M. Heijne, CERN, Geneva, Switzerland

November 1982

* This research was supported by the U. S. Department of Energy: Contract No. DE-AC02-76CH00016.

CHARGE COLLECTION IN SILICON STRIP DETECTORS

H. W. Kraner, R.Beuttenmuller, T. Ludlam, A. L. Hanson, K. W. Jones, and V. Radeka
Brookhaven National Laboratory

E. H. M. Heijne, CERN

Introduction

The use of position sensitive silicon detectors as very high resolution tracking devices in high energy physics experiments has been a subject of intense development over the past few years (1). Typical applications call for the detection of minimum ionizing particles with position measurement accuracy of 10μm in each detector plane. The most straightforward detector geometry is that in which one of the collecting electrodes is subdivided into closely spaced strips, giving a high degree of segmentation in one coordinate. Each strip may be read out as a separate detection element, or, alternatively, resistive and/or capacitive coupling between adjacent strips may be exploited to interpolate the position via charge division measurements(2,3). With readout techniques that couple several strips, the number of readout channels can, in principle, be reduced by large factors without sacrificing the intrinsic position accuracy. The testing of individual strip properties and charge division between strips has been carried out with minimum ionizing particles or beams for the most part except in one case which used alpha particles scans (2). This paper describes the use of a highly collimated MeV proton beam for studies of the position sensing properties of representative one dimensional strip detectors.

The segmentation of a one dimensional readout can be miniaturized until basic processes or inherent detector limitations divide the collected charge over two or more contact electrodes. Segmentation much below the projected size of the collected charge cloud will not improve the centroid definition of the event. Diffusion at the very least will govern the "size" of the collected event and can be estimated theoretically. Anomalies to the collection process such as uneven depletion depths or variable collecting fields should also be investigated.

Detectors

Silicon surface barrier detectors have been prepared from both n and p type silicon of nominal resistivities between 5 and 10 kΩ cm. The detector thickness chosen is 300 μm which is a compromise between sufficiently large signal (energy loss) from minimum ionizing particles and low multiple scattering. Signals of 80-130 keV are therefore expected from minimum ionizing particles in this thickness. 2.5 Mev protons used in this study are completely stopped having a range of 60μm in silicon (4) and produce a greatersignal than for minumum ionizing particles; signal levels are not a limiting factor in these studies. Surface barrier detectors are a relatively simple junction detector type with which to initiate charge collection studies. Gold on n-type silicon is the common p+ contact with aluminum used as the "back" or n contact. The aluminum contact can also be rectifying on p-type silicon which permits a common technology for each material type. Wafers approximately 1 cm in diameter were mounted with a p- and n-type epoxy system (5) on 1/16" G-10 epoxy board. A strip pattern shown in Figure 1 is applied to the Al contact by a positive photoresist technology. The strips are grouped as follows: six with 200 μm pitch, six with 100 μm pitch and six with 40 μm pitch. The aluminum contact covers about half of the area between the strips. Contact from the aluminum strips to the readout lines of the mother board is made by ultrasonic wedge bonding with ".001" Al wire. The "pads" or large areas above and below the strip patterns are also Al contacts and serve to keep planar field geometry.

Several satisfactory devices have been made with nominal 7 kΩ Komatsu n-type material which will be taken as representative. Some variability in the Al (n+) contact affected the maximum allowed over voltage. Results with one such n-type device, called 40N, will be primarily described.

300 μm thick detectors deplete in the neighborhood of 60-70 V as determined by capacitance measurements on the large area "pad" contacts. Interelectrode resistances can be measured between strips as a function of applied bias and varies between 50 KΩ at 40 V (about two-thirds undepleted) to > 10 MΩ at over deplection at 80V. These values pertain to the 100 μm pitch strips on n-type material in which depletion proceeds towards the strip contact. Clearly, this value is sufficiently large so that an external resistance divider for charge division (<50 KΩ) would not be significantlyshunted by the detector itself.

The technique of using photo-lithographic techniques with positive (and initially negative) resist have been remarkably straight-forward. The wafer is etched surface treated and mounted in the G-10 board with "n-type" epoxy. Resist is spun on the aluminum side following aluminum and gold metallization. After resist exposure with uv light and post baking, the unexposed resist is easily stripped with acetone and the inter-strip aluminum is removed with ≈ 10% NaOH. Following thorough washing the residual resist is removed and ultrasonic wire bonding is used to attach the strips to external contacts on the G-10 board. Leakage currents are generally in the several microamp range which is sufficiently low for these studies.

Collimated Proton Beam

Figure 2 is a schematic of a beam line at the BNL 3.5 MV electrostatic research accelerator which enables a collimated proton beam to be brought into the laboratory through an arrangement of differential pumping. The specifics of this facility have been described by Shroy et al.,(6). A number of well- developed "microbeams" exist world-wide (7) having both focused and collimated charged particle beams for elemental and distributional analysis. This system which permits the beam to emerge into the laboratory is particularly useful for detector development as it permits the strip detector to be easily positioned without breaking vacuum. A stepping motor drives the detector across the beam in increments as small as 5 μm/step.

A 2.5 MeV proton beam was used, the size of which was defined by the final collimator at the exit of the beam pipe. When the collimated beam is used for proton induced x-ray analysis (PIXE), great care must be taken to use a collimator of low Z material that both stops the beam and does not itself produce spurious x-rays that can either scatter or themselves fluoresce materials near the sample. Because the charged particles themselves were of interest in detector tests, this constraint was removed and 12 to 20 μm diameter platinum electron microscope apertures were used that produced the beam definition shown in Figure 3. A beam of ≈ 20 μm in extent is measured by stepping a thin nickel foil edge into the beam and counting K_α x-rays with the Si(Li) x-ray spectrometer. Although some beam halo undoubtedly exists, much of the residual counts when the Ni foil is not intercepted by the beam must be due to Ni x-rays fluoresced by the Pt L x-rays from the collimator edge (an effect of no import for the proton beam studies). The stepping calibration is easily checked by the scan of a 200 mesh Cu grid in which Cu K x-rays are counted as a function of position. The step size of ≈ 10 μm/step was verified for this particular setting of stepping motor pulses. The proton beam current was integrated at the end of the beam pipe and has been judged sufficiently stable so that emergent beam is directly proportional to it. Scans of strip detectors are taken for equal integrated beam intensities.

Figure 4 is a schematic of the experimental arrangement of the strip detector and with respect to the beam. The detector is in proper scale as noted by the 100 μm width bar. The range of 2.5 MeV protons in silicon is ≈ 60 μm and the beam width is taken as 20 μm; the beam is ≈ 7° off perpendicular (see Figure 2) to allow fluoresced x-rays to be viewed from a back angle without interference from the beam end. The beam can be injected into either side of the detector which emphasizes the extremes of charge collection that are averaged for particles that fully traverse the detector thickness. The beam may be considered nearly cylindrical over its range as lateral straggling amounts to only a few μm(4). The lateral definition of the beam, noted in Figure 3 was measured ≈ 4 mm from the beam pipe end at very nearly the identical position of the detector. The strips shown on Figure 4 extend in the "long direction" outward from the plane of the paper. Two Ortec 142 preamplifiers sensed adjacent strips whose signals were introduced into separate ADCs for display as both one- and two-dimensional spectra on a Nuclear Data 6600 data collection system. Time constants of 0.5 μsec were used in conventional linear amplifiers; the preamp bias loads were modified to 2.2 MΩ and grounded at the preamp; bias was supplied to the detector from the gold p+ continuous contact. The "pads" and all unused strip contacts were grounded.

The data collection system permitted one dimensional pulse height spectra from each strip to be collected as well as the "correlated" or coincident events between each strip viewed on the two-dimensional display. The number of counts in each type of display could be determined and will be discussed. Further, a scope display of linear pulses from each strip outputwas found useful to judge where the beam was positioned, its rate, and to observe possible anomalies.

Results

A two-dimensional spectrum from the n-type detector 40N which suggests extremely good position sensitivity is shown in Figure 5. Protons are injected into the gold side with the bias at 60 V, just under depletion so that some diffusion of the electrons sensed by two 100 μm pitch contacts can occur. The zero of the display is in the upper right corner. The steps or separation between each spectrum is 20 μm. One strip axis is the far edge of the display; the other axis is along the right edge. Singles spectra are not displayed on the axes in this system, but will be displayed separately. The diagonal between the two strip axes is essentially full energy deposition on each axis and represents ≈ 100 μm distance between center of the strips; the centroid of correlated events is well defined in both position (Δx on the diagonal) and energy (Δr in radial dispersion). The "track" of the beam position across this diagonal, (the sum of collected charge) appears linear over most of the range. The diagonal is slightly reduced approaching each axis as some charge is shared with the next adjacent strip. If viewed radially, one might estimate a positional resolution of ≈ 10 μm FWHM for the diagonal dispersion. Although some consideration has been given to using surface barrier strip detectors in an undepleted condition, several problems such as material non-uniformity can be anticipated with this condition. The complementary runs for protons incident on the strip side for the undepleted detector at 50 and 64 V bias, slightly under depletion are shown in Figures 6a and 6b, respectively. At 50 V bias with some spreading of charge onto both strips possible in the undepleted material, a considerable population of correlated events are observed; some charge loss is also shown as the diagonal is compressed towards the origin. The effect of slower rising pulses from the series resistance of undepleted material not being fully integrated within the amplifier time constants cannot be ruled out as a mechanism for apparent charge loss (ballistic deficit) in this case. The next scan at 64 V, more nearly depleted, shows fewer correlated events and suggests the "either-or" effect of charge collection on the strip side of the detector. This effect is clearly shown Figure 7 in the comparison of singles spectra from each strip for the detector run very nearly at depletion when the proton beam is at the intermediate position between strips. Collection of charge is clearly on one strip or the other depending on which side of the median between the strips, particle incidence occurs. This effect is enhanced for operation with biases at or above depletion.

In contrast to the one dimensional spectrum for proton incidence on the strip side, the singles spectra for gold side incidence at a bias below depletion, Figure 8, shows continuous charge sharing, which reinforces the observations of the 2D spectrum in Figure 5.

At depletion and above, proton incidence on the gold side, Figure 9, 85 V bias, behaves much more like strip side incidence with events appearing only on one strip or the other; qualitatively, little diffusion really occurs to give a wide range of shared events over many intermediate beam positions. The two middle - or median - positions of Figure 9 show truly shared events; from 20 μm on either side of the median position, most events are essentially collected by a single strip. Similarly, for proton incidence on the strip side, at depletion, collection primarily by the individual strips is emphasized. Figure 10 compares the singles spectra in each of adjacent 100 μm pitch 50 μm wide strips showing distinct single strip collection for all scansbut the median position (c). Figure 11 is the 2D spectrum and shows really correlated events only for the intermediate position,(c).

Figure 12 summarizes charge sharing for strip and gold side proton incidence at depletion. In the double count fraction, the data "points" are bars which indicate the 20 μm beam spread that should be qualitatively deconvoluted from the data. At the top, strip side incidence, the presence of shared events for only the median position is obvious compared with the lower portion for gold-side incidence. In the lower curve, the dotted line suggests the real trend of the data at the higher values of beam position; the strip used in this direction was the end strip of the group of six which retained some sensitivity into the void between strip groups. In the lower curves for smaller values of beam position, however, it is possible to suggest that a spreading or sharing of charge in addition to the 20 μm beam resolution is present. This may be a real effect of diffusion which will be discussed.

Figure 13 shows again the effect of bias on population and distribution of correlated events for proton incidence on the gold side at a median position for biases of 100, 85, 60 and 40 V where depletion has occurred at 85 V. The vertical count scales are identical for each run except for the 2D spectrum at 40 V which is compressed by a factor of 2.5. At 40 V, one has the best centroid definition but clear charge loss shown from the singles spectra.The loss of correlated events with increasing bias between 60 and 100 V bias is clear as is the predominance of singles strip collection (note the middle column). A difference in material resistivity as noted by somewhat different depletion voltages for each "pad" contact- opposite sides of the wafer - may also account for the movement of the charge collection from strip B (right side column, singles) to strip A (middle column) as depletion occurs from 60 to 85 V and beyond depletion.

Figure 14 summarizes the bias effect quantitatively, wherein the event fraction for both singles and doubles (correlated) is plotted. For these results, the counts in each spectra are integrated above a reasonable noise threshold; the fraction is formed as a ratio to "all" events which is the sum of singles events less the number of correlated events. The trend from correlated doubles to singles between 60 and 100 V is clear as is the migration of singles events from strip "C" to strip "B" (the center column in the previous figure) with increasing bias. The values at 40 V may be suspect and are not included in the trend as some sharing between other adjacent strips may well occur at rather low bias.

A peculiar effect in strip charge collection was observed for proton incidence on the strip near the median position between both the 100 μm and 200 μm pitch strips with the detector bias near depletion at 60 V. The scope traces of the linear amplifier outputs of each strip, were observed with the scope triggered by the particular strip to which the beam was closest (but still at a near median position). The correlated pulses from the strip furthest from the beam were found to be inverted as shown in the middle two scope pictures of Figure 15. In the third and fourth scope pictures, the trigger is now in the upper trace as the scan moves towards that strip. Negative pulses are then observed on the lower trace in symmetry with the observation of the second from top picture. In this case, there are 80 μm between each picture, the step numbers having differences of two (1, 3, 5, 7, e.g.). This effect was enhanced by reducing the proton energy to 1.2 MeV (≈ 20 μm range) and rescanning the area between 200 μm pitch strips producing thepronounced negative pulses shown in Figure 16. Whereas the p+ aluminum electrode collects electrons, an opposite polarity pulse in an adjacent electrode correlated within ≈ 1 μsec must be due to the injection of electrons rather than collection. Charge injection has been observed near contacts for highly ionizing particles as well as muons (8) in which a positively charged region around the track is present momentarily after collection of the more mobile electrons. A local area of concentrated positive charge can probably overcome the negative fixed charge in the p+ interface and allow electron injection from the metallic strip. This effect was also observed in median positions between 100 μm pitch strips operated at or above depletion. The size of the negative pulses appeared to increase with beam running time on a particular spot indicating a possible effect of radiation damage. The beam current was then increased substantially and the advent of negative pulses from the adjacent electrode was further verified. Because hole trapping is a common deleterious effect of charged particle or neutron damage, furtherer reduction of hole collection capability from this surface region is surely expected to enhance the injection field.

Discussion

Before considering particular aspects of these results, it is well to reemphasize that the use of a collimated heavy particle beam directed ≈ 60 μm into one side or the other of a 300 μm thick silicon detector is a distinct overstatement of the effects of minimum ionizing particles which traverse the entire detector and no effort has been taken here to "integrate" or average any effect in order to better simulate minimum ionizing particles. The unique capabilities and convenience of using this beam in air at rates which permit good statistics enable device charge collection studies which would be difficult or impossible with minimum ionizing particles. With the proton beam the ionization is

produced in the vicinity of either contact electrode, thus these studies emphasize contact properties. With minimum ionizing particles the ionization in the bulk of the depletion region dominates, and may obscure the contact properties. Although surface properties may be less significant in high energy physics applications, they are not insignificant to an understanding of the detector, itself. Of course, with minimum ionizing particles the charge produced by ionization is smaller (about 2.4×10^4 electrons for detector thickness of 300 μm) than with 2.5 MeV protons ($\approx 7 \times 10^5$ electrons). This comparison has to be taken into account in the readout and preamplifier design.

a. Diffusion Figures 6 and 7, summarized in Figure 12, upper portion, note the loss of charge for particles which are at the median position for proton incidence on the strip side. In contrast, some diffusion must occur to for particles incident on the gold side where collected electrons traverse the full detector thickness according to Figure 9 and summarized in the lower portion of Figure 12. One dimensional diffusion produces a near-gaussian distribution with standard deviation given by (9):

$$\sigma = \bar{r} = \sqrt{2Dt} \qquad (1)$$

where D is the diffusion coefficient
and t is the drift time

using the Einstein relation, $D = kT\mu/q$, where μ is the carrier moblity and q is the electronic charge,

$$\sigma = \sqrt{2kT\mu t/q} \qquad (2)$$

The drift time t is the thickness of the depletion depth or device w, divided by a drift velocity. In turn, the drift velocity is given by the mobility field product for a non-saturated velocity condition. If a constant electric field, V/w, across its active depth is assumed, then we have the simple, limiting condition for both electrons and holes:

$$\sigma = \sqrt{2kTw^2/qV} = \sigma_o \qquad (3)$$

If the field, E, in a 300 μm thick silicon junction were constant and was given by $50V/300 \times 10^{-4}cm$, the relationship above would yield σ=10μm. However the field in a step junction device is not constant but linearly decreasing from the junction contact. Therefore:

$$t = \int_0^w dx/v(x) = (1/\mu)\int_0^w dx/E(x) \qquad (4)$$

The field E(x) can be described in terms of the applied bias V_d required for depletion of a thickness w_d by:

$$E(x) = \frac{2V_d}{w_d}(1 - x/w_d) \qquad (5)$$

The depletion depth w_d and depletion voltage are uniquely related through the material resistivity and a constant according to the familiar relationship $w_d = k(\rho V)^{1/2}$ which may be used as an additional descriptive parameter in (5). As given above, this relationship holds for positions within the depleteion region up to a value w_d which may encompass the actual device thickness. In other terms, equation (5) holds for fields just above depletion and beyond where the value of depletion depth w_d exceeds the device dimension. For the case of under depletion it is difficult to define a drift time in the undepleted region where presumably little field exists. In actuality, the undepleted material represents a relativiely low series resistance, however a small field must exist across it to complete charge collection. It is difficult to model this field given only the boundary conditions of the potential at the junction contact and the material resistivity and even more hazardous to suggest a field that might practically exist. Therefore, the diffusion estimate for an undepleted detector will not be considered. For biases above depletion, however, equations (4) and (5) may be used to find:

$$\sigma(x) = \sqrt{\frac{2kTw_d^2}{qV_d}\left\{-\frac{\ln(1-x/w_d)}{2}\right\}^{1/2}} \qquad (6)$$

where $0 \leq x < w_d$.

If values of x/w_d approach one, letting the device thickness approach the depletion depth or in letting the applied bias b nearly only that of depletion, the second factor in (6) approaches a factor of two over σ_o which can judged to be the effect of the linearly decreasing field at depletion contrasted with the diffusion expected for a constant field. The broadening of the adjacent electrode response for full thickness drift, protons into the gold side, shown in the lower portion of Figure 12 is at most of the order of 20 μm, consistent with the above considerations.

b. Charge Injection from an Adjacent Contact. Without going into complex analysis and delineation of the perturbation of the space charge region near a strip contact which would be necessary to fully understand injection from an adjacent contact, a first step may be taken to compare the local charge generated by the event with the indogenous fixed charge of the n-type material. A 2.5 MeV proton stopping in a volume of silicon defined by the track length of 60 m and an area defined by the track length of 60 μm and an area defined by several microns (≈4μm) lateral straggling produces 0.7×10^{15} electron-hole pairs per cm^3 in this volume. Assuming the electrons are swept out directly and some dilution of the hole concentration occurs, one might more realistically compare the instantaneous positive charge value of $10^{14}/cm^3$ with the fixed space charge value for 7KΩ-cm material of $7 \times 10^{11}/cm^3$, which indicates a considerable space charge anomaly and perturbation to the local field. Injection per se will be governed by the amount of fixed positive charge a under the aluminum interface. The degree to which the aluminum strip acts as a blocking contact, however these numbers suggest at least that a substantial irregularity in the space charge in the silicon can occur very close to the electron supply from the contact. Injection in a configuration not dissimilar has also been observed by Heijne (8).

Another facet of injection from an adjacent contact which has been observed is a distinct increase in size of the negative pulse or injected charge with irradiation time at the particular interstrip site. This effect was easily tested by several runs in the median area between 100 μm pitch aluminum strips in which the beam current was increased to produce proton rates at 2.5 MeV ≈ 10^4/sec. In periods as short as 300 sec., distinct increases in injected charge were observed at positions somewhat off the median where initially negative pulses were not observed. Considering that image effects usually involve hole trapping, this rate effect certainly also serves to retain positive charge near the contact electrode.

To Summarize:

1. A collimated MeV proton beam in the laboratory has proved useful and convenient to examine some details of charge collection in segmented silicon function detectors - "strip" detectors. Because fluoresced x-rays are not important to this measurement a further reduction in emergent beam size could be effected by finer, heavy metal collimaters, yielding beams down to ≈ 3-5 μm. Adequate beam then limited by beam line vibration, e.g. is easily attainable suggesting further studies in the range of expected beam diffusion sizes.

2. Simple surface barrier devices with a representative test pattern have been produced by contact lithography.

3. Negative pulses from adjacent electrodes have been observed and are attributed to charge injection. This effect should not be of great concern for minimum ionizing particles.

4. Diffusion of charge is at most ≈ 10 μm for representative device parameters and must be somewhat less for particles which fully traverse the active depth. The difference between linear and constant fields in the structure should be recognized.

5. Operation at full depletion obviates problems of material inhomogeneity. Therefore in large scale experiments it is hard to imagine not operating these detectors fully depleted.

6. The strip pitch for fine resolution of fully depleted detectors (σ<10μm) should be of the order of 2σ. Larger pitch would introduce nonlinearity in the position measurement and smaller pitch would not improve the centroid definition.

Acknowledgements

It is a pleasure to thank Robert E. Mills who artfully produced small and stable beam currents from the 3.5 MV Research Accelerator. We thank F. J. Walter for a helpful and illuminating discussion.

References

1. Pisa Meeting on Miniaturization of Detectors for High Energy Physics, 18-21 September 1980; to be published in Plenum Press.

Workshop on Developments in Solid State Detectors for Elementary Particle Physics, CERN/EF/0439H/EH/ed., 5 May 1981.

E. H. M. Heijne, Nucl. Inst. & Meth. 178, 331 (1980).

S. R. Amendolia, et al., Physica Scripta 23, 671 (1981), Nucl. Inst. & Meth. 176, 457 (1980).

Silicon Detectors in High Energy Physics, Proceedings of a Workshop held at Fermilab, Oct. 15-16, (1981), T. Ferbel, U. of Rochester, ed.

E. Belau, R. Klanner, et al, MPI-PAE/Exp.El.104, June (1982).

2. J. B. A. England, B. D. Hyams, L. Hubbeling, J. C. Vermuelen and P. Werlhammer, Nucl. Inst. & Meth. 196, 149 (1982). Also CERN-EP/80-219, 3 Dec. 1980.

3. E. Laegsgaard, Nucl. Inst. & Meth. 162, 73 (1978).

4. U. Littmark and J. F. Ziegler, Handbook of Range Distributions of Energetic Ions in All Elements, Volume 6, Pergamon Press, N.Y. (1980).

5. R. J. Fox and C. J. Borkowski, I.R.E., Trans. Nucl. Sci., NS-9, 213 (1962).

6. R. E. Shroy, W. W. Kraner, K. W. Jones, Nucl. Inst. & Meth. 157, 163 (1978).

7. J. A. Cookson, Nucl. Inst. & Meth. 181, 115 (1981); Nucl. Inst. & Meth. 165, 477 (1979).

F. Bosch, et al, Science 199, 765 (1978).

C. J. Maggiore, Scanning Electron Microscopy, Volume 7, (1980), Om Tohari, ed., IITRI and LA-UR 80-390.

P. Horowitz and L. Grodzins, Science 189, 795 (1975).

8. E. H. M. Heijne, personal communication.

9. Peter Rice-Evans, Spark, Streamer, Proportional and Drift Chambers, The Richelliue Press, London (1974).

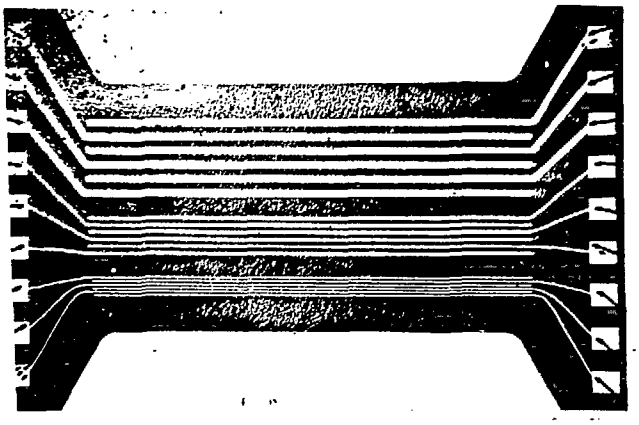

Figure 1. The strip pattern of the aluminum n contact for the silicon detectors used in this experiment. The light areas above and below the strips are large contact areas ("pads") used to better define the entire contact potential. Wire bands are in place. The groups of strips have 40, 100 and 200 μm pitch.

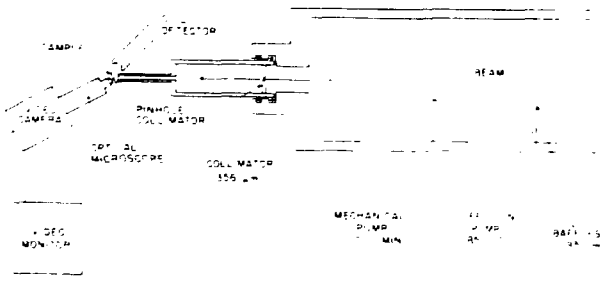

Figure 2. End of beam line for collimated MeV proton beam at BNL 3.5 MV Research Accelerator showing differential pumping arrangement which permits a windowless exit for the beam into the laboratory ([7]). Positioning of ancillary equipment such as detectors and monitors may vary.

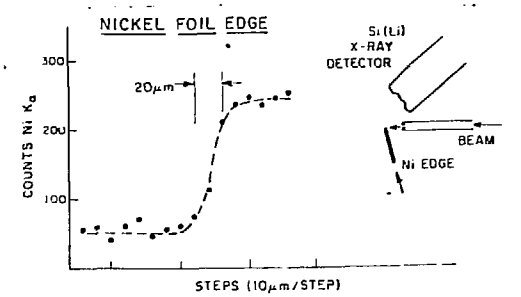

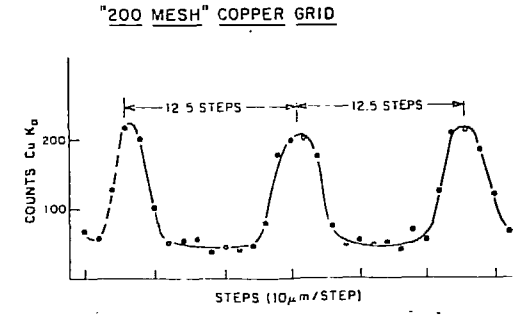

Figure 3. Calibration of beam size and stepping increments for collimator and drives used in this experiment. The collimator was a nominal 12 μm diameter platinum electron microscope aperture, ≈ 125 μm thick. The number of steps between copper mesh wires which are spaced 125 μm apart agrees with the assumption of 10 μm/step.

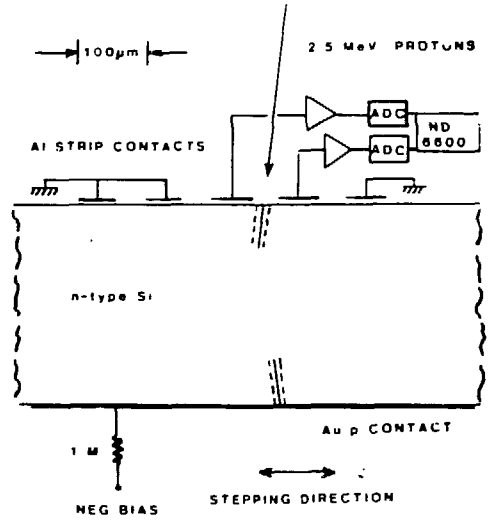

Figure 4. Schematic of experimental arrangement for an n-type silicon strip detector. Linear signals from two adjacent strips are routed to a one- and two-dimensional Nuclear Data 6600 data collection system. The detector is moved relative to the beam in a direction perpendicular to the length of the strips. The detector itself and beam definition within the detector for a particular scan position are to scale; the remainder of the figure is schematic. The volume of deposited charge for both strip side and gold side incidence is shown.

Figure 5 The two-dimensional spectra of shared or "correlated" events when protons are incident on the gold (back) side of the detector which is based at 60 V, just under depletion. Two 100 μm pitch strips are sensed and the step size between each position is 20 μm.

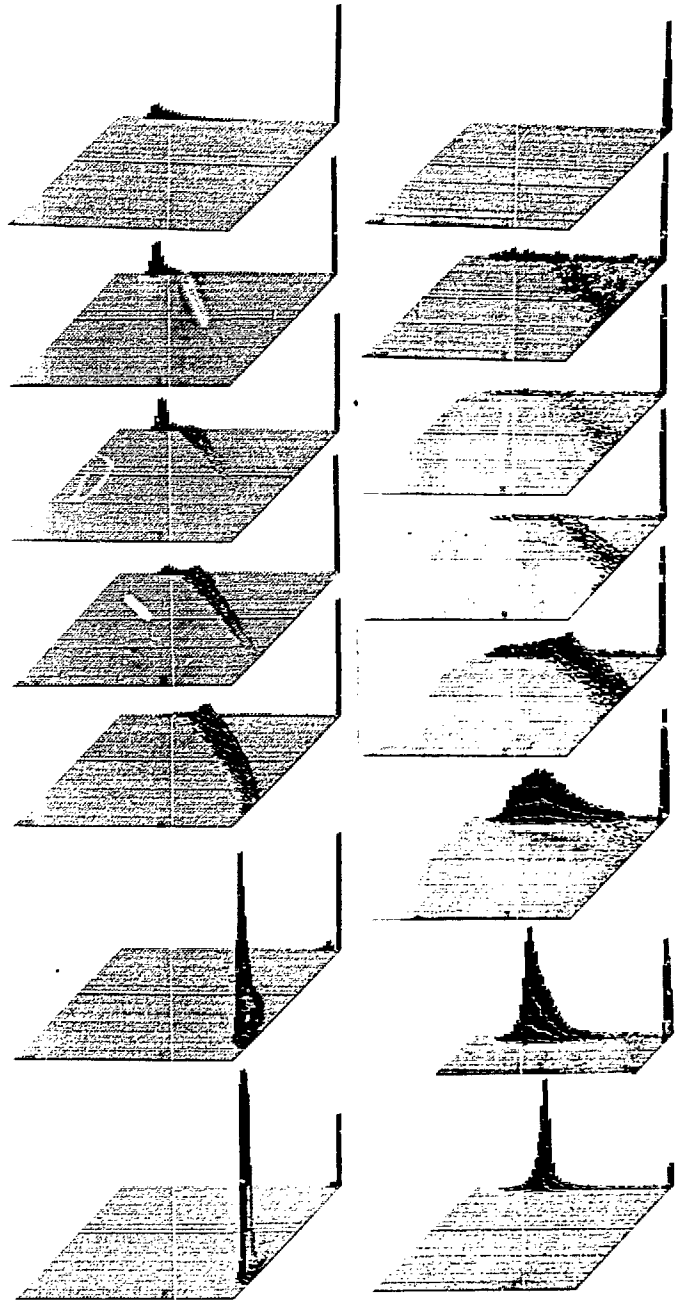

Figure 6. Two dimensional spectra of correlated events betwen 100 μm pitch strips of n-type silicon detector for proton incidence on strip side where the steps run from directly "on" one strip to the other in steps of 20 μm. 6(a) on the left is with 50 V bias and 6(b), right, for 64 V bias, just under depletion.

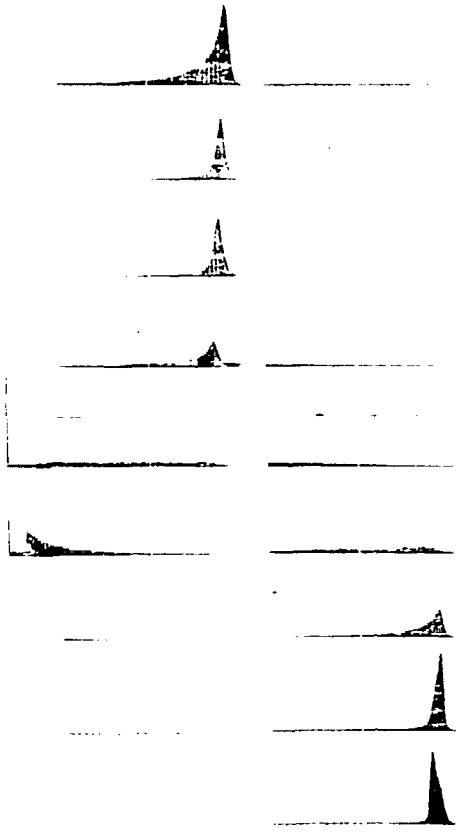

Figure 7. Singles spectra of adjacent 100 μm strips in n-type silicon detector with protons incident on the strip side. 20 μm steps between each position are used and one should note an offset energy zero for both right and left side strip spectra should be noted. The effect of one strip (left side) having all counts, neither in the middle, and all counts finally in the right column strip is clear. The bias was 50 V, under depletion, in this case.

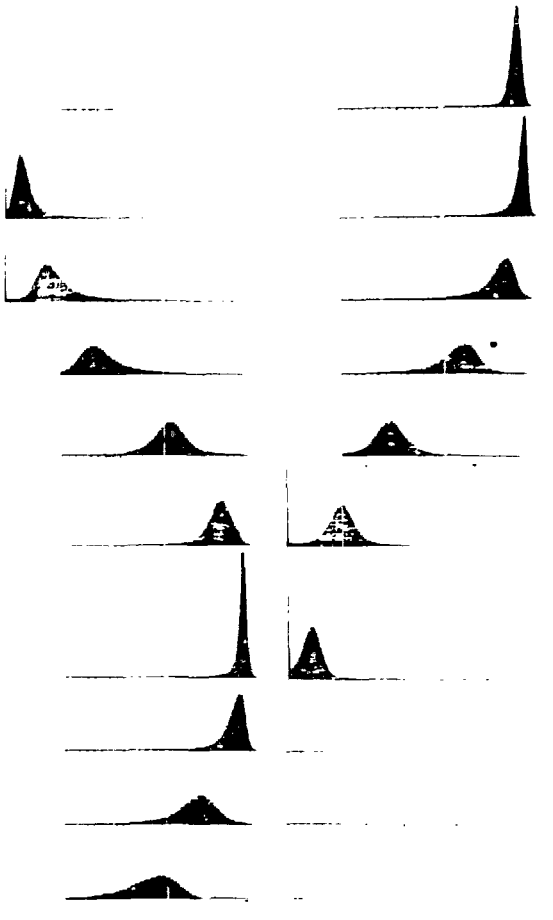

Figure 8. Singles spectra for adjacent 100 μm pitch strips for proton incidence on the gold side with bias at 60 V, under depletion, for the n-type silicon detector. Note the zero energy offsets which are used in the spectra when the beam is underlying one strip or another.

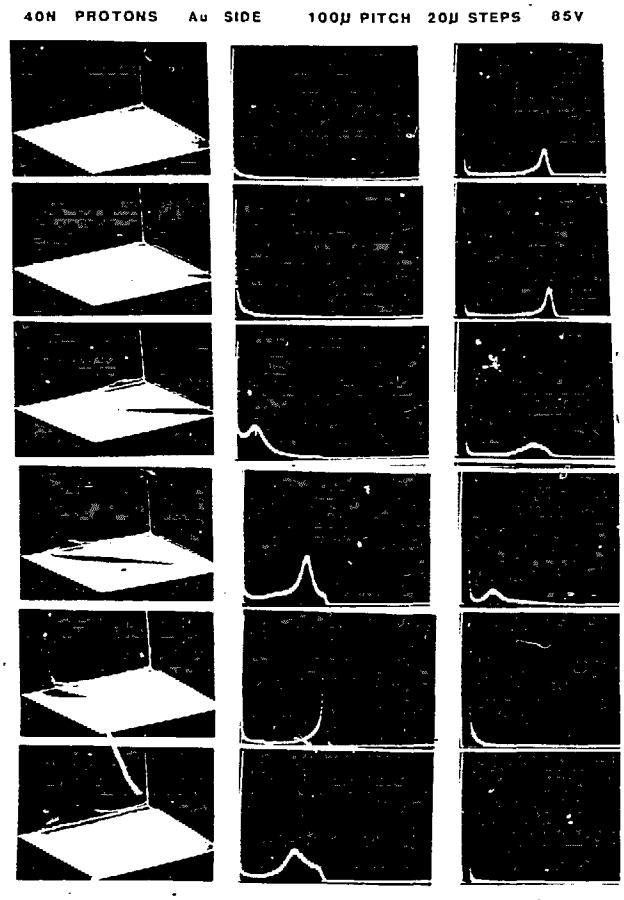

Figure 9. Both two dimensional correlated events spectra (left column) and singles spectra (middle and right column) for 100 μm pitch strips for protons incident on gold side with bias above depletion, 85V The step size between each spectrum group is 20 μm.

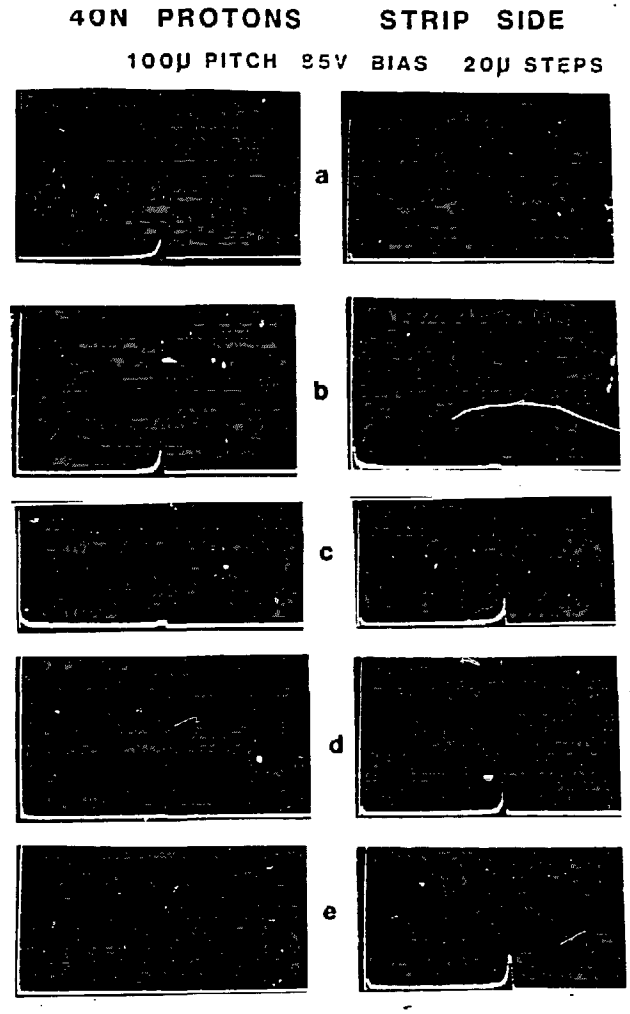

Figure 10. Singles spectra from 100 μm pitch strips for protons incident on strip side with detector bias over depletion, 85 V.

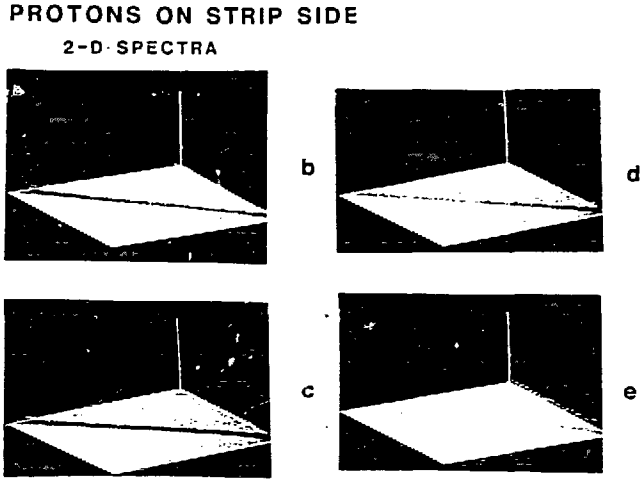

Figure 11. Two-dimensional spectra from 100 μm pitch strips for proton incident on strip side with detector bias over depletion, 85 V.

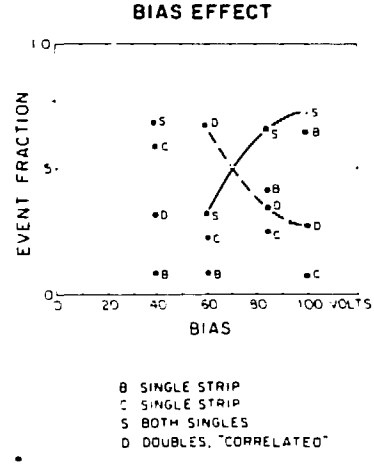

Figure 14. Quantitative summary of the bias effect for 100 μm pitch strips of the n-type silicon detector with protons incident on the gold side. The data are from the runs shown in Figure 13.

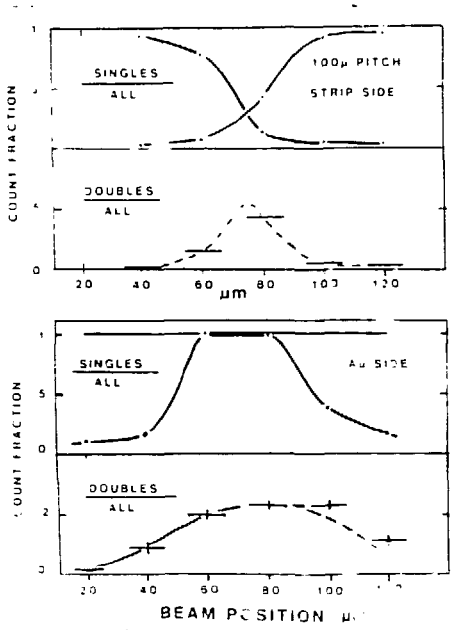

Figure 12. Summary of singles and correlated events from 100 μm pitch strips in the n-type silicon detector expressed quantitatively as a fraction of the full number of events recorded per beam position. The normalization for singles is that for the clear position of the beam directly over (or under) one of the sensed strips.

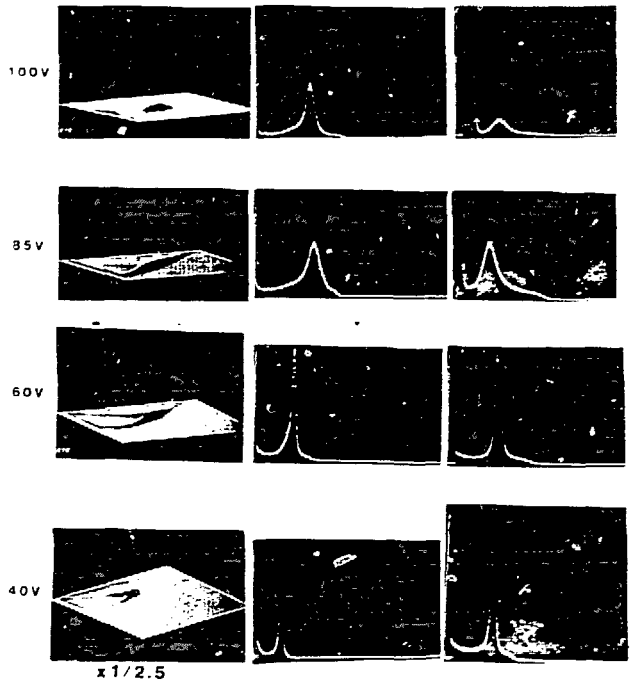

Figure 13. The effect of bias on the singles and two-dimensional spectra for 100 μm pitch strips with protons incident on the gold side. The vertical scale of the 2D spectrum at 40 V is compressed by 2.5; otherwise all scales are identical.

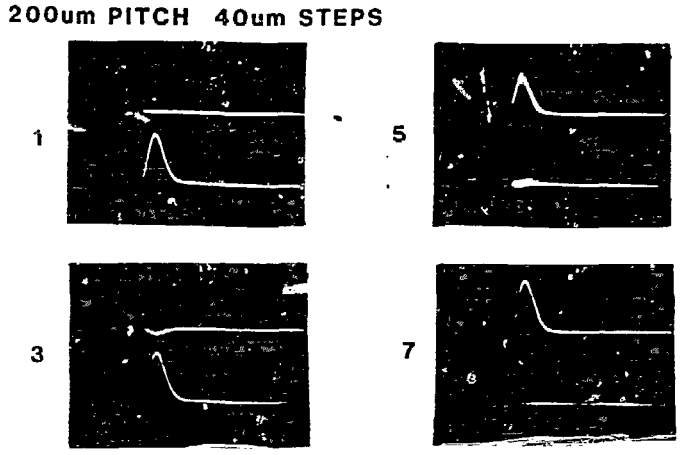

Figure 15. Scope traces of the linear amplifier output signals from each of adjacent 200 μm pitch strips on the n-type detector. 2.5 MeV protons were incident on the strip side of the detector. The step size was 40 μm and every second step is shown. In 1 and 3 the scope trigger was taken from the lower trace; on 5 and 7, the trigger was by the upper trace.

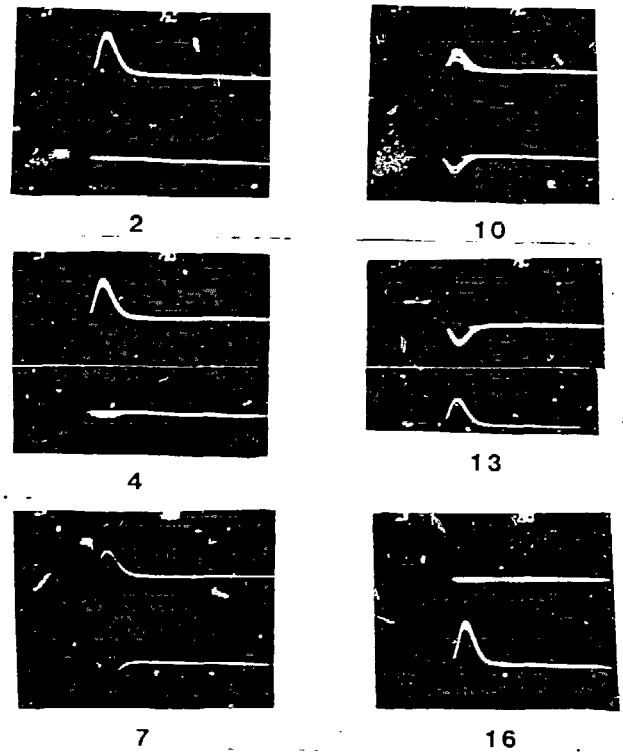

Figure 16. Scope traces of the linear amplifier output signals from each of adjacent 200 μm pitch strips on the n-type detector. Gains are identical to those of Figure 15, however the proton energy has been reduced to ≈ 1.2 MeV which reduces the proton range and enhances the negative pulse effect. The scope is triggered by the upper trace for steps 2, 4 and 7 and by the lower trace for 10, 13 and 16. Each numerical step increment (1, 2, 3, etc.) is 20 μm.